NEXT-TO-LEADING ORDER DETERMINATION OF FRAGMENTATION FUNCTIONS

L. Bourhis[3], M. Fontannaz[2], J.Ph. Guillet[1], M. Werlen[1]

1. *Laboratoire de Physique Théorique LAPTH,* *
   B.P. 110, F-74941 Annecy-le-Vieux Cedex, France

2. *Laboratoire de Physique Théorique* †
   Université de Paris XI, Bâtiment 210, F-91405 Orsay Cedex, France

3. *Department of Theoretical Physics*
   South Road, Durham City DH1 3LE, United Kingdom

Abstract

We analyse LEP and PETRA data on single inclusive charged hadron cross-sections to establish new sets of Next-to-Leading order Fragmentation Functions. Data on hadro-production of large-$p_\perp$ hadrons are also used to constrain the gluon Fragmentation Function. We carry out a critical comparison with other NLO parametrizations.

hep-ph/0009101
Durham 00/28
LAPTH-802/00
LPT-Orsay/99/94
September 2000

*UMR 5108 du CNRS, associée à l'Université de Savoie.
†Unité mixte de recherche (CNRS) UMR 8627

1 Introduction

Inclusive hadron production in various processes gives the possibility to carry out quantitative tests of the QCD-improved parton model. The essential property of QCD cross-sections which allows comparisons between various processes is the factorization property. Indeed thanks to the factorization theorem [1], the cross-sections are written as convolutions of basic building blocks, such as the quark and gluon distributions in the incoming hadrons, the hard subprocesses describing the large-angle scattering of partons, and the fragmentation functions of quarks and gluons into hadrons. The parton distributions and fragmentation functions can be defined in a universal way. Therefore these distributions measured in one reaction can be used to perform predictions for another reaction. On the other hand, the subprocess cross-section is entirely calculable in perturbative QCD, the only free parameter being Λ_{QCD}.

Many processes involving fragmentation functions can be related in this manner. Among them the best studied are the e^+e^--annihilation into hadrons $e^+e^- \to hX$, the observation of hadrons in DIS experiments $\ell p \to \ell hX$, and the hadro- and photo-production of large-$p_\perp$ hadrons $h_a h_b \to h_c X$ and $\gamma h_a \to h_c X$. Clearly quantitative studies of these reactions can only be performed if sets of next-to-leading order (NLO) fragmentation functions are available.

While there are several sets of parton distribution functions for the proton and the pion, mainly extracted from DIS data, few sets of fragmentation functions exist. It is only recently that many precise data on the hadron energy spectrum in e^+e^--annihilation became available from LEP experiments, completing those obtained at lower energy at DESY, SLAC and TRISTAN. The accuracy of these data is remarkable ; they should allow a determination of fragmentation functions with a precision which approaches that obtained in the parton distribution functions. A first step towards a NLO analysis of fragmentation functions has been done by Chiappetta et al. (CGGRW collaboration) [2], who studied the fragmentation into π^0. As LEP data did not exist at that time, these authors also made a detailed study of large-$p_\perp$ π^0 cross-sections, measured by ISR experiments and the UA2 collaboration, in order to constrain their parametrizations. LEP data was used by Binnewies, Kniehl and Kramer (BKK coll.), in association with lower energy results

of PEP and PETRA, to determine the parton fragmentation into charged pions and kaons, and into neutral kaons [3, 4]. From these results and the measured ratio p/π, they indirectly obtained fragmentation functions for charged particles[‡].

We pursue these studies and propose parametrizations[§] of the parton fragmentation functions into charged particles by directly analyzing the corresponding e^+e^- data. The interest of such functions is that they can be used in all reactions in which there is no particle identification. On the other hand this set of fragmentation functions can be compared with the BKK set, thus offering an estimation of the "theoretical error" embedded in the parametrizations and which comes from various theoretical assumptions used to perform fits to data. We shall see, in section 3, that the gluon fragmentation function is poorly constrained by e^+e^- data. Therefore we shall complete our anlysis by that of the hadron-production of large-$p_\perp$ charged hadrons, a reaction which is sensitive to the gluon fragmentation function.

This paper is organized as follows. In section 2, we present the theoretical expressions we use to calculate the single inclusive hadron cross-section in e^+e^--annihilation, and we describe the parametrization of the non-perturbative boundary conditions associated to the DGLAP evolution equations for the fragmentation functions. We also pay attention to an improved choice of the renormalization and factorization scales. In section 3, we describe the fits to LEP and PETRA data and discuss our results. Then we study, in section 4, the constraints put on the gluon fragmentation function by large-$p_\perp$ hadron production. We conclude in section 5.

2 Single Inclusive Cross Section in e^+e^- Annihilation

In the QCD-improved parton model, the single inclusive cross-section is given by the expression

$$\frac{dN^h}{dz} = \frac{1}{\sigma_{tot}} \frac{d\sigma(e^+e^- \to hX)}{dz} = \sum_{a=q,\bar{q},g} \int_z^1 \frac{dy}{y} D_a^h\left(y, M^2\right) \frac{1}{\sigma_{tot}} \frac{d\sigma_a}{dv}\left(v = \frac{z}{y}, \mu^2, M^2, Q^2\right) . \tag{1}$$

[‡]During the completion of this work, two new papers on fragmentation functions apppeared[5, 6]. We shall briefely comment on them.

[§]These fragmentation functions are available on request (guillet@lapp.in2p3.fr).

The longitudinal variables $z = \dfrac{2p_h \cdot Q}{Q^2}$ and $v = \dfrac{2p_a \cdot Q}{Q^2}$ measure the fraction of the energy $\sqrt{Q^2}$, available in the e^+e^- CMS, carried away by the hadron h and the parton a. The fragmentation functions $D_a(u, M^2)$ describe the non-perturbative transition of parton a into hadron h. Only the dependence on the factorization scale M is perturbatively calculable and given by the DGLAP evolution equation

$$M^2 \ \frac{\partial D_a^h(M^2)}{\partial M^2} = \sum_a P_{ba}^T \otimes D_b^h(M^2) \tag{2}$$

where $\otimes$ indicates a convolution : $(f \otimes g)(x) = \int_0^1 dy \ dv \ f(y) \ g(v) \ \delta(yv - x)$. The time-like kernels are expansions in $\alpha_s(M^2)$

$$P_{ba}^T(M^2) = \frac{\alpha_s}{2\pi}(M^2) \ P_{ba}^{(0)} + \left(\frac{\alpha_s}{2\pi}(M^2)\right)^2 \ P_{ba}^{T(1)} + \cdots \tag{3}$$

In this paper we work at the NLO approximation and when solving (2), we use the NLO kernels $P_{ba}^{T(1)}$ [7, 8]. Eq. (2) can be solved more easily by working in moment-space. We use this formalism here as well as a computer code written by P. Nason [9].

The hard subprocess cross-section $d\sigma_a/dv$ describes the production of a parton a in e^+e^--annihilation. (We consider only the sum of the transverse and longitudinal cross sections). It is given by an expansion in $\alpha_s(\mu^2)$ where μ^2 is the renormalization scale :

$$\frac{d\sigma_a}{dv}(v, \mu^2, M^2, Q^2) = \frac{d\sigma_a^{(0)}}{dv}(v, Q^2) + \frac{\alpha_s}{2\pi}(\mu^2)\frac{d\sigma_a^{(1)}}{dv}(v, M^2, Q^2) + \cdots \tag{4}$$

We use expressions calculated at order $\alpha_s(\mu^2)$ [10]. For the total cross-section σ_{tot} we also use the $O(\alpha_s)$ expression[¶] :

$$\frac{1}{\sigma_{tot}} = \frac{1}{N_c \frac{4\pi\alpha^2}{3Q^2} \sum\limits_{i=1}^{N_f} e_{q_i}^2 \left(1 + \frac{\alpha_s(\mu^2)}{\pi}\right)} \simeq \frac{1}{\sigma^{Born}} \left(1 - \frac{\alpha_s}{\pi}(\mu^2)\right) \quad . \tag{5}$$

Throughout this paper, we work at NLO accuracy and do not take into account the NNLO expressions calculated by Rijken and van Neerven [12]. Several reasons impose this choice. First, the full NNLO correction is not known ; the 3-loop DGLAP kernel is missing. Second, we shall use these fragmentation functions in

[¶]Expressions of σ^{Born} which also contain the Z^0 contribution may be found in ref. [11, 12].

the calculation of cross section for which only NLO expressions are available (for instance large-$p_\perp$ inclusive cross sections) ; it appears more coherent to also use NLO parametrizations of the fragmentation functions. One must also notice that the NLLO corrections to the e^+e^- inclusive cross section are very small when z is not too close to zero or one [12]. In this paper, we study data in the range $.12 \leq z \lesssim .9$, and for $z \simeq .9$ the experimental errors are larger than the NLLO corrections.

In order to neglect kinematical higher twists of order $m^2/\vec{p}^2$ where m is a hadron mass and $\vec{p}$ its momentum, we restrict the z-range ($z \sim 2|\vec{p}|/\sqrt{Q^2}$) studied by the condition $z \gtrsim .12$. This condition also allows us to neglect "MLLA" effects [13] which show up at small z and are not included in the NLO formalism described in this section.

On the other hand the $\mathcal{O}(\alpha_s^2)$ corrections to the longitudinal cross section $d\sigma_L/dz$ calculated in [12] are non-negligible. However we will not use this cross section to constrain to gluon fragmentation functions $D_g(z, Q^2)$, because data at large z ($z \gtrsim .4$) is scarce and not very precise.

Finally let us mention that we work in the $\overline{MS}$ scheme and that we use massless expressions for the DGLAP kernels and the hard cross sections. However we take into account the bottom threshold by starting the evolution of the b-quark fragmentation function at $M^2 = m_b^2$.

The cross-section (1) depends on arbitrary scales which show up in the course of the theoretical calculations : the renormalization scale μ and the factorization scale M. They must be chosen of the order of $\sqrt{Q^2}$, but their precise value cannot be determined by any fondamental rule. However several approaches exist which propose prescriptions to improve the choice of these scales ; we adopt here the "Principle of Minimum Sensitivity" criterion [14]. At the order $\alpha_s(\mu^2)$ at which $d\sigma_a/dv$ is calculated (LO calculation in $\alpha_s(\mu^2)$), no prescription constrains μ and we choose $\mu = M$. Then we fix M using the PMS criterion

$$M^2 \, \frac{\partial}{\partial M^2} \left(\frac{dN}{dz} \right) \Bigg|_{M=M_{opt}} = 0 \quad . \tag{6}$$

We find by a numerical study of (6) that M^2_{opt} is much smaller than Q^2. In a large range in z, we have $M_{opt} \simeq \sqrt{Q^2}/5$. However at small values of z ($z \lesssim .2$), M_{opt} starts to increase to values as large as $\sqrt{Q^2}$. At Mark II [15] energy ($\sqrt{Q^2} = 29$ GeV),

the PMS criterion does not work for $z \gtrsim .3$; there is no solution of equation (6). Because of this result, we shall only study data with $\sqrt{Q^2} \gtrsim 35$ GeV. This leads us to discard PEP data.

As already discussed, the non-perturbative physics of the cross-section (1) is entirely contained in the fragmentation functions $D_a^h(y, M^2)$. The perturbative evolution of these fragmentation functions is given by eq. (2) which must be supplemented by a non-perturbative initial condition. The latter is fixed by the y-behavior of the fragmentation functions at an initial scale Q_0^2. As we are interested in the use of the fragmentation functions in reactions where the scale M can be of the order of a few GeV (hadro- or photoproduction of large-$p_\perp$ particles), we start the evolution at a small value of M, namely $M^2 = Q_0^2 = 2$ GeV^2 ($M^2 = m_b^2$ for D_b). At this value of M, we fix the shape of the fragmentation function by using a simple and standard parametrization

$$
\begin{aligned}
D_g\left(y, Q_0^2\right) &= N_g (1-y)^{\beta_g}\ y^{\alpha_g} \\
D_u\left(y, Q_0^2\right) &= \left(N_u (1-y)^{\beta_u} + \bar{N}_u (1-y)^{\bar{\beta}_u}\right) y^{\alpha_u} \\
D_{d+s}\left(y, Q_0^2\right) &= \left(N_{d+s} (1-y)^{\beta_{d+s}} + \bar{N}_{d+s} (1-y)^{\bar{\beta}_{d+s}}\right) y^{\alpha_u} \\
D_c\left(y, Q_0^2\right) &= N_c (1-y)^{\beta_c}\ y^{\alpha_c} \\
D_b\left(y, m_b^2\right) &= N_b (1-y)^{\beta_b} y^{\alpha_b} \quad .
\end{aligned}
\tag{7}
$$

Let us say a few words on the theoretical and "experimental" reasons for this parametrization. First we notice that the e^+e^--annihilation cross-section is only sensitive to the sum $D_{d+s} = D_d + D_s$. So we are not able to determine D_d and D_s separately. This degeneracy could be lifted by looking at DIS data, or at data on the production of large-$p_\perp$ particles. However the large -$p_\perp$ production cross-sections, at UA1 and UA2 energy, are sensitive to the gluon fragmentation function, and very little to the d-quark fragmentation function. Therefore in this paper, we will not give separate descriptions of the d- and s-quark fragmentation functions. On the other hand, in order to reduce the number of free parameters of the fit, we assume that the small-z behaviour of the light quarks are the same : $\alpha_u = \alpha_d = \alpha_s$.

By performing a fit to e^+e^- data (see next section), we observed that several parameters of the input (7) are strongly correlated with each other. For instance

N_g, α_g and β_g are strongly correlated, as well as N_u, $\bar{N}_u$, β_u, and α_u, $\bar{N}_{d+s}$ and N_g. The b-parameters also are strongly correlated with each other. Because of these correlations, the fitting procedure is very lengthy and we cannot obtain a positive definite error matrix. Therefore we proceed in two steps. First we perform a fit with all parameters free. Then, in order to reduce the correlations, we fix some parameters to the values obtained in the first fit. This will be discussed in detail in the next section.

We also observed a strong correlation between the gluon parameters and the functional shape of the input distribution $D_{d+s}(y, Q_0^2)$. A simple form of the type $N(1-y)^\beta y^\alpha$ leads to a gluon fragmentation function which is in disagreement with large-$p_\perp$ charged particle data of UA1 [16]. Thus we use more flexible shapes, as those of formula (7), in order to try to decorrelate, as far as possible, gluon and light quark parameters.

In the present paper, we do not intend to determine from data the value of $\Lambda_{\overline{MS}}$. This value might be sensitive to power corrections [11, 17] and such an analysis is beyond the scope of this work. Here we use a fixed value of $\Lambda^{(4)}_{\overline{MS}}$: $\Lambda_{\overline{MS}} = 300$ MeV, in agreement with the CTEQ4M [18] and MRST [19] distribution functions. One must note that this value is quite in agreement with the new value obtained in Ref[5] in a fit to e^+e^- annihilation data.

3 Analysis of e^+e^--annihilation data

Inclusive charged particle data from CELLO [20] at $\sqrt{Q^2}$ =35 GeV, from TASSO [21] at $\sqrt{Q^2}$ =44 GeV, from AMY [22] at $\sqrt{Q^2}$ =58 GeV, from DELPHI [23] and SLD [24] at $\sqrt{Q^2}$ =91.2 GeV are used in the fits. To constrain the flavor dependent parameters, the uds, c and b flavor enriched samples from ALEPH [17], DELPHI [25] and OPAL [26] are used. A b enriched sample from DELPHI [23] has also been included.

To take into account the experimental systematics errors, avoiding the treatment of correlated errors, the following procedure has been adopted: the normalization errors are not included in the χ^2 evaluation but a normalization for each experiment is taken as a parameter of the fit allowed to vary within 3 standard deviations of the quoted experimental uncertainty. For ALEPH, as we use enriched samples

in the fit, we do not used the all charged data which has correlated errors [17]. The normalization of ALEPH ligth quark sample is kept fixed to 1., while a common normalization N_{OPAL} ($N_{DELPHI\ 94}$, N_{DELPHI}) is allowed for all OPAL samples (DELPHI 94 samples [23], DELPHI [25]).

Using the program Minuit [27], we performed a first fit to data, obtaining a reasonable result with $\chi^2 = 215$ for 217 data points and 25 parameters. In particular the data normalization factors are very close to one. As discussed in the preceding section, we observe strong correlations between the parameters and the error matrix is not positive definite.

The strong correlation between β_u and $\bar{\beta}_u$, β_{d+s} and $\bar{\beta}_{d+s}$ leads us to fix the diffferences $\bar{\beta}_u - \beta_u$ and $\bar{\beta}_{d+s} - \beta_{d+s}$ to the results of the first fit namely $\bar{\beta}_u - \beta_u = 1.15$ and $\bar{\beta}_{d+s} - \beta_{d+s} = 3.6$. Similarly, we fix $\alpha_g = 0$ and $\alpha_b = -1.7$. The χ^2 is now 204 for 217 points and 14 parameters. But the fit is not yet converging and the error matrix is not positive definite. The source of this problem lies in the remaining strong correlation between N_b and β_b. Fixing also N_b and β_b we eventually get a convergent fit. Relaxing the condition $\alpha_g = 0$ also lead to a convergent fit with a positive definite error matrix and the following parameters for the non-perturbative inputs at $Q_0^2 = 2$ GeV^2. (The data normalization factors N_i are also fixed to the values obtained in the first fit)

$$
\begin{array}{ll}
D_g(y, Q_0^2) & = 2.11(1-y)^{1.37} y^{-.71} \\
D_u(y, Q_0^2) & = \left(3.45(1-y)^{2.25} - 0.955(1-y)^{3.4}\right) y^{-0.68} \\
D_{d+s}(y, Q_0^2) & = \left(0.95(1-y)^{.945} + 10.43(1-y)^{4.545}\right) y^{-0.68} \\
D_c(y, Q_0^2) & = 5.15(1-y)^{3.87} y^{-0.78} \\
D_b(y, Q_0^2) & = 0.897(1-y)^{3.7} y^{-1.7} \\
N_{ALEPH\ b} & = 1.03 \\
N_{ALEPH\ c} & = 1.014 \\
N_{OPAL} & = 0.999 \\
N_{DELPHI\ 94} & = 1.0006 \\
N_{DELPHI} & = 1.0005 \\
N_{SLD} & = 0.9998 \\
N_{CELLO} & = 1.0055 \\
N_{AMY} & = 1.0117 \\
N_{TASSO} & = 0.9835
\end{array}
\tag{8}
$$

The corresponding χ^2 is 201 for 217 data points and 13 parameters.

A technical discussion of errors and correlation matrices is given in appendix 1.

Here we just quote the results of a full analysis (MINOS [27],[28]) on the parameter N_g. We obtain a variation of χ^2 by one unit when increasing (decreasing) the value of N_g to 5.25 (1.10), leaving the other parameteres free. These alternative fits are studied and used in section 4 where we discuss large-pt data.

One notices that the gluon input is flat, comparable to the light quark fragmentation functions. However e^+e^- inclusive cross sections poorly constrain the gluon fragmentation function and the gluon parameters are determined with a large errror. The gluon fragmentation function corresponds to an $\mathcal{O}(\alpha_s)$ correction to the Born cross section, and it is quite sensitive to the functional forms of the light quark inputs. Therefore we cannot draw any physical conclusion from this result. However, it turns out that the gluon (8) gives a good description of the UA1 large-$p_\perp$ data. This point will be developed in section 4.

It is interesting to compare our fit to the corresponding data by using ratios and linear scales which exhibit agreements or disagreement more clearly. The experimental error is the quadratic sum of statistical and systematic errors.

Let us start the discussion by the b-enriched cross sections (Fig. 1,2). The agreement is generally good, but one notices at large z some discrepancies between the various data sets which might indicate that the systematic errors are underestimated. The light and c-quark theoretical cross sections and data are displayed in Fig. 3, Fig. 4 and Fig. 5. CELLO and TASSO data (Fig. 5) are mainly sensitive to the u and c-quark fragmentation functions, whereas light-quark enriched LEP sample (ALEPH uds, DELPHI, OPAL uds, DELPHI uds) are sensitive to the d and s-quark fragmentation function. Here one also notices some dispersion of the LEP light quark data at large z. The all charged data from DELPHI and SLD, also included in the fits, are shown in Fig. 6.

In fig. 7 we compare the result of our fit with the BKK fragmentation function [3, 4] at $Q^2 = 10000$ GeV^2. The two parametrizations are in reasonable agreement for $z \lesssim .6$; however one must keep in mind that BKK studied pion and kaon cross sections, and indirectly all charged cross sections (see below). In fig. 8 we display ratios of fragmentation functions on a linear scale in order to compare them more closely.

The u-quark and b-quark fragmentation functions are harder in BKK. The effect could be understood partly as follows: the ratio of proton/pion cross section, inspired

from data (fig. 5 of [29]), has been given the form $0.195 - 1.35(y - 0.35)^2$ by BKK. However, the high y part of this form, not constrained by data, is negative above 0.7 ; as a result their fit to all charged hadrons up to $y = 0.8$ will have a tendency to enlarge some of the quark fragmentation functions in the large-y region. On the other hand, the s-quark fragmentation function is constrained by kaon production in BKK approach and cannot be directly compared to our parametrization which does not distinguish between s-quark and d-quark ; from Fig. 8 one can deduce that the ratio $(d + s)/(d + s)_{BKK}$ increases from 1.1 at $y \simeq .1$ to 1.5 at $y \simeq .8$. The gluon fragmentation functions have different shapes but, as already discussed, they are not very well constrained by e^+e^- annihilation data.

The BKK collaboration also performed a direct fit of ALEPH charged hadron data and we can compare the parametrizations given in the thesis of J. Binnewies [30] with our results. The ratios of the fragmentation functions are displayed in Fig. 9. The agreement between the quark distributions is reasonable for $.1 \lesssim z \lesssim .6$. For $z > .6$, our fragmentation functions are much larger than those of ref. [30]. One reason for this difference may come from the choice of the data. We choose to fit all LEP data. As a result, our cross sections overshoot ALEPH data in the large-z domain. On the other hand Binnewies' parametrization slightly undershoots ALEPH data. Let us also notice that in ref. [30] ALEPH data is studied only in the range $z \leq .8$. Therefore we may expect differences with our parametrizations for $z \gtrsim .8$.

Finally, one must also keep in mind that we used "optimized" cross sections (expression (6)) whereas BKK used the scale $M^2 = Q^2$. Moreover the bottom threshold is set at $M^2 = 4m_b^2$ by the BKK collaboration whereas we have $M^2 = m_b^2$. This may introduce slight differences between the parametrizations.

The author of Ref. [6] also compared his parametrization with the BKK one and observed disagreements for $z > .5$. The behaviors of the ratios shown in Fig. 8 have similarities with those shown in Ref. [6] for the quark fragmentation functions. But one notes a strong disagreement for the gluon fragmentation function which is very small for $z > .5$ in Ref. [6] compared to the BKK parametrization. Such a behavior seems to be in contradiction with the large-pt UA1 data discussed in the next section. where an 83% (54%) contribution to the cross section is due to the gluon fragmentation at $p_T = 5GeV/c$ ($p_T = 21.9GeV/c$).

4 Analysis of large-$p_\perp$ production rate

The determination of the gluon fragmentation function $D_g(z, Q^2)$ from the inclusive e^+e^- cross section is not very precise. The gluon contribution to the cross section is a NLO effect, and, during the fitting procedure, we found that the gluon parameters were quite sensitive to the functional form at Q_0^2 chosen for the quark distributions.

A better constraint could come from the longitudinal cross section $d\sigma_L/dz$. But data at large z, where we want to determine $D_g(z, Q^2)$, is rare and not accurate. Therefore we turn to hadroproduction of large-$p_\perp$ hadron which constrains the fragmentation function in the large-z region ($z \simeq .7$). In hadronic collisions at small $x_\perp = 2p_\perp/\sqrt{s}$, the contribution to the cross section involving the gluon fragmentation function are large, and the theoretical predictions are quite sensitive to them.

Data from the UA1 collaboration on charge hadrons at large $p_\perp$ (1 GeV $\lesssim p_\perp \lesssim$ 20 GeV) precisely cover this kinematical domain. For the theoretical predictions, we use the code of ref. [31] which includes NLO corrections. The quark and gluon distribution are from MRST-2 [19] and $\Lambda_{\overline{MS}} = 300$ MeV. The factorization and renormalization scales are set equal to $p_\perp/2$; a choice which is dictated by the stability of the cross section when the scales vary around $p_\perp/2$ [32]. Our results for the region $p_\perp > 5$ GeV/c where we trust higher order QCD correction are compared with data in fig. 10. The slope and normalization are well reproduced, theory slightly overshooting data. The contribution to the cross section due to the gluon fragmentation is important, going from 83% to 54% from $p_T = 5GeV/c$ to $p_T = 21.9GeV/c$.

We can try to improve the agreement between large-$p_\perp$ data and theory by modifying the gluon parameters (8) within the allowed error range. With $N_g = 5.25$ on the one hand, and $N_g = 1.1$ on the other hand, we obtain two new sets of parameters and a χ^2 value increased by one unity : $\chi^2 = 202$.

$$\begin{array}{ll} D_g(y, Q_0^2) & = 5.25(1-y)^{1.87} y^{-0.03} \\ D_u(y, Q_0^2) & = (3.46(1-y)^{2.26} - 1.4(1-y)^{3.31})\, y^{-0.77} \\ D_{d+s}(y, Q_0^2) & = (0.959(1-y)^{0.95} + 8.86(1-y)^{4.21})\, y^{-0.77} \\ D_c(y, Q_0^2) & = 4.07(1-y)^{3.68} y^{-0.91} \\ D_b(y, Q_0^2) & = 0.897(1-y)^{3.72} y^{-1.7} \end{array} \qquad (9)$$

$$
\begin{array}{ll}
D_g(y,Q_0^2) & = 1.1(1-y)^{1.02}y^{-1.19} \\
D_u(y,Q_0^2) & = \left(3.32(1-y)^{2.24} - 0.5(1-y)^{3.39}\right) y^{-0.62} \\
D_{d+s}(y,Q_0^2) & = \left(0.93(1-y)^{0.94} - 0.5(1-y)^{4.54}\right) y^{-0.62} \\
D_c(y,Q_0^2) & = 6.37(1-y)^{4.06}y^{-0.68} \\
D_b(y,Q_0^2) & = 0.897(1-y)^{3.72}y^{-1.7}
\end{array}
\tag{10}
$$

The corresponding fragmentation functions are compared to those obtained from the input (8) in Fig. 11 and 12 for $Q^2 = 10000$ GeV^2. We note a change in the gluon shape which is important at large z. Unfortunately the large-$p_\perp$ cross section tests the fragmentation functions in the domain $z \simeq .7$ where the change is small, and we do not expect a substantial modification of the large-$p_\perp$ cross section. This point is verified in Fig. 13 and 14 which shows only a very slight improvement of the ratio data/theory. Therefore we conclude that the 3 sets of parameters (8), (9) and (10) are compatible with UA1 data.

5 Conclusion

In this paper we have performed a NLO analysis of e^+e^- annihilation into charged hadrons data in order to determine a new set of fragmentation functions. Although many LEP data are now available, including samples with enhanced content in heavy quarks, we find that it is impossible to obtain a convergent fit when using three (or five for the u-quark) free parameters to characterize the input shapes of the quark and gluon fragmentation functions. There are strong correlations between the parameters and we do not obtain a positive definite error matrix.

Fixing some of the strongly correlated parameters to values obtained in a fit characterized by a good χ^2, we succeed in obtaining a positive definite error matrix. The overall agreement with data is quite good. Comparing our parametrizations of the fragmentation functions with those obtained by the BKK collaboration [4], we note several important discrepancies, especially in the large-z domain. These discrepancies should come from the assumption made by the BKK collaboration on the large-z behavior of the charged hadron cross sections. A better agreement is reached with the results of ref. [30] in which charged cross sections are also studied. But in the large-z region, one again notes important discrepancies. One explanation of the discrepancy could be the fact that we use sets of data extending to larger z-values than those fitted in [30].

This point also emphasizes the necessity to carefully treat the large-z region and to resum the large logarithms in the theoretical expressions. In this work this is done through the optimized scales which should also be used in the calculation of other reactions making use of the present parametrization.

We also test the gluon fragmentation function in large-$p_\perp$ hadronic collisions. We find that 3 sets of fragmentation functions allowed by e^+e^- data within one standard deviation and differing in the gluon shape lead to very similar predictions for large-$p_\perp$ cross sections at the $Sp\bar{p}S$ energy. The overall agreement with UA1 data is quite good.

6 Appendix

Uncertainties on the parameters of the fit (8) can be roughly estimated with the error matrix using the curvature at the minimum and assuming a parabolic shape [27], [28]: the results are given on Table 1 where the parabolic errors quoted take into account the effects due to parameter correlations. These errors should be taken as lower limits on the errors, as some parameters, which may be correlated to the ones estimated, have been fixed in the fitting procedure. The results of a full MINOS analysis (non-parabolic chisquare) [27, 28], following the χ^2 out of the minimum and finding where it corresponds to $\Delta_{\chi^2} = 1$ is given on Table 2.

Table 1: Errors on the parameters and correlation

par.	error	correlation with											
		α_g	β_g	N_{d+s}	α_u	β_{d+s}	N_u	$\bar{N}_u$	β_u	$\bar{N}_{d+s}$	N_c	α_c	β_c
N_g	1.49	0.98	0.97	0.11	-0.66	0.10	-0.003	-0.16	-0.03	-0.71	-0.6	-0.6	-0.5
α_g	0.53		0.90	0.04	-0.75	0.05	0.01	-0.19	-0.02	-0.78	-0.6	-0.6	-0.5
β_g	0.40			0.22	-0.52	0.18	-0.02	-0.12	-0.05	-0.58	-0.5	-0.5	-0.5
N_{d+s}	0.16				0.20	0.97	-0.57	0.57	-0.49	0.10	0.08	0.12	-0.03
α_u	0.09					0.16	-0.35	0.55	-0.32	0.98	0.29	0.36	0.14
β_{d+s}	0.09						-0.62	0.58	-0.57	0.08	0.09	0.12	0.01
N_u	1.4							-0.97	0.97	-0.30	0.0	-0.04	0.07
$\bar{N}_u$	2.0								-0.92	0.49	0.05	0.11	-0.05
β_u	0.25									-0.30	-0.04	-0.06	0.01
$\bar{N}_{d+s}$	1.8										0.30	0.35	0.16
N_c	1.77											0.99	0.95
α_c	0.17												0.90
β_c	0.33												

Table 2: Uncertainties on the parameters

parameter	parabolic error	negative error	positive error
$N_g = 2.12$	1.49	-1.02	+3.1
$\alpha_g = -0.71$	0.53	-0.51	+0.70
$\beta_g = 1.37$	0.40	-0.38	+0.51
$N_{d+s} = 0.948$	0.157	-0.15	+0.17
$\alpha_u = -0.684$	0.099	-0.11	+0.098
$\beta_{d+s} = 0.944$	0.091	-0.090	+0.096
$N_u = 3.435$	1.40	-1.56	+1.35
$\bar{N}_u = -0.956$	2.01	-1.94	+2.19
$\beta_u = 2.26$	0.25	-0.33	+0.22
$\bar{N}_{d+s} = 10.43$	1.83	-1.95	+1.93
$N_c = 5.15$	1.77	-1.54	+2.26
$\alpha_c = -0.789$	0.177	-0.184	+0.186
$\beta_c = 3.87$	0.33	-0.33	+0.35

References

[1] D. Amati, R. Petronzio, G. Veneziano, Nucl. Phys. **B140** (1978) 54, **B146** (1978) 29.
R. K. Ellis, M. Georgi, M. Machacek, H.D. Politzer, G.C. Ross, Nucl. Phys. **B152** (1979) 285.

[2] P. Chiappetta, M. Greco, J.-Ph. Guillet, S. Rolli, M. Werlen, Nucl. Phys. **B412** (1994) 3.

[3] J. Binnewies, B.A. Kniehl, G. Kramer, Z. Phys. **B65** (1995) 471.

[4] J. Binnewies, B.A. Kniehl, G. Kramer, Phys. Rev. **D52** (1995) 4947.

[5] B.A. Kniehl, G. Kramer, B. Poetter, DESY preprint 00-053, hep-ph/0003297.

[6] S. Kretzer, Dortmund preprint TH 00/04, hep-ph/0003177 v2

[7] G. Curci, W. Furmanski, R. Petronzio, Nucl. Phys. **B175** (1980) 27.
W. Furmanski, R. Petronzio, Phys. Lett. **B97** (1980) 435.

[8] E.G. Floratos, C .Kounas, R. Lacaze, Nucl. Phys. **B192** (1981) 417.

[9] P. Nason, private communication.

[10] G. Altarelli, R. K. Ellis, G. Martinelli, S. Y. Pi, Nucl. Phys. **B160** (1979) 301.
R. Baier and K. Fey, Z. Phys. **C2** (1979) 339.

[11] P. Nason and B. R. Webber, Nucl. Phys. **B421** (1994) 473.

[12] P.J. Rijken and W.L. van Neerven, Nucl. Phys. **B387** (1997) 233.

[13] Ya.I. Azimov, Yu.L. Dokshitzer, V.A. Khoze, S.I. Troyan, Z. Phys. **C27** (1985) 65 ; ibid. **C31** (1986) 213.

[14] P.M. Stevenson, Phys. Rev. **D23** (1981) 2916.
H.D. Politzer, P.M. Stevenson, Nucl. Phys. **B286** (1987) 509.

[15] Mark II collaboration, A. Petersen et al., Phys. Rev. **D37** (1988) 1.

[16] UA1 collaboration, G. Bocquet et al., Phys. Lett. **B366** (1998) 434 and private communication from H. Dibbon.

[17] ALEPH collaboration, D. Buskulic et al., Phys. Lett. **B357** (1995) 487; erratum ibid **B354** (1995) 247;
C. Padilla, Ph.D. thesis, Univ. of Barcelona, 1995 (unpublished) and private communication.

[18] CTEQ collaboration, H.L. Lai et al., Phys. Rev. **D55** (1997) 1280.

[19] A.D. Martin, R.G. Roberts, W.J. Stirling and R.S. Thorne, Eur. Phys. J. **C14** (2000) 133.

[20] O. Podobrin, Ph.D. thesis, Univ. of Hamburg, 1992, unpublished (the data can be found on table 4 of [33]).

[21] TASSO collaboration, W. Braunschweig et al., Z. Phys. **C47** (1990) 187.

[22] AMY collaboration, Y.K Li et al., Phys. Rev. **D41** (1990) 2675.

[23] DELPHI collaboration, P. Abreu et al., Eur.Phys.J.**C5** (1998) 585.

[24] SLD collaboration, K. Abe et al., Phys. Rev. **D59** (1999) 052001.

[25] DELPHI collaboration, P. Abreu et al., Phys. Lett. **B398** (1997) 194.

[26] OPAL collaboration, K. Ackerstaff et al., Eur. Phys. J. **C7** (1999) 369.

[27] F. James, MINUIT, CERN program library D506; F. James and M. Roos, Comp. Phys. Comm. **10** (1975) 343.

[28] W.T. Eadie, D. Drijard, F. James, M. Ross and B. Sadoulet. Statistical Methods in Experimental Physics. North Holland, 1971.

[29] ALEPH collaboration, D. Buskulic et al., Z. Phys. **C66** (1995) 355.

[30] J. Binnewies, Desy 97-128 (hep-ph/9707269).

[31] F. Aversa, P. Chiappetta, M. Greco, J.-Ph. Guillet, Phys. Lett. **B211** (1988) 465; Nucl. Phys. **B327** (1989) 105.

[32] P. Aurenche, M. Fontannaz, J.-Ph. Guillet, B.A. Kniehl, M. Werlen, Eur. Phys. J. **C13** (2000) 347.

[33] DELPHI collaboration, P. Abreu et al., Phys. Lett. **B311** (1993) 408.

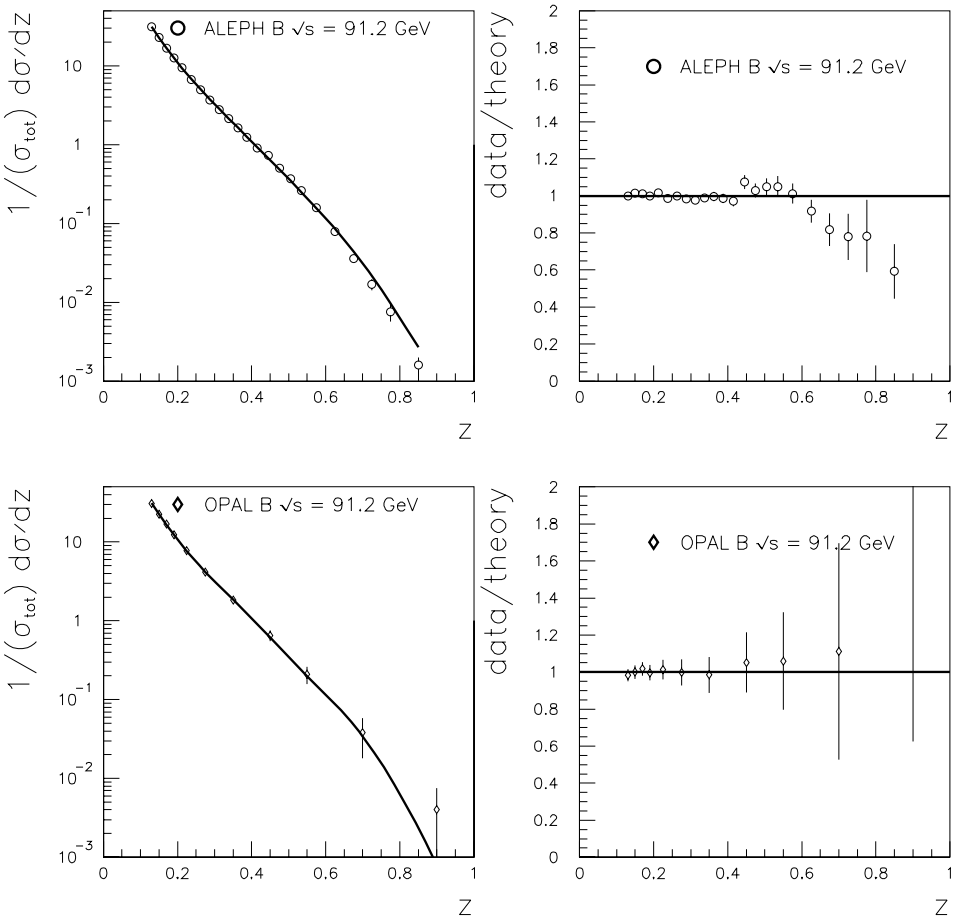

Figure 1: NLO inclusive charged particle production in $e^+e^- \to bX$ collisions at $\sqrt{s} = 91.2$ GeV with optimized scales and with fragmentation functions obtained here (formula 8) compared to data of the ALEPH [17] and OPAL collaboration [26].

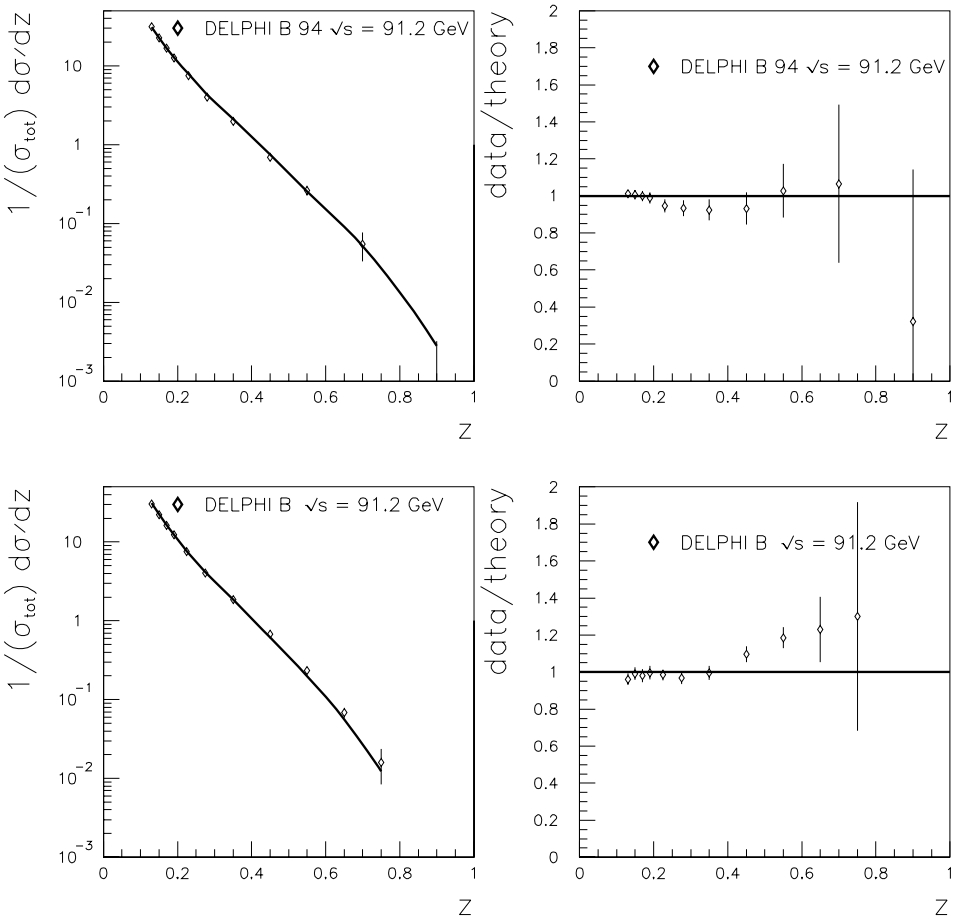

Figure 2: NLO inclusive charged particle production in $e^+e^- \to bX$ collisions at $\sqrt{s} = 91.2$ GeV with optimized scales and with fragmentation functions obtained here (formula 8) compared to data of the DELPHI collaboration taken in 1994 (top) [23] and in 1991-1993 [25].

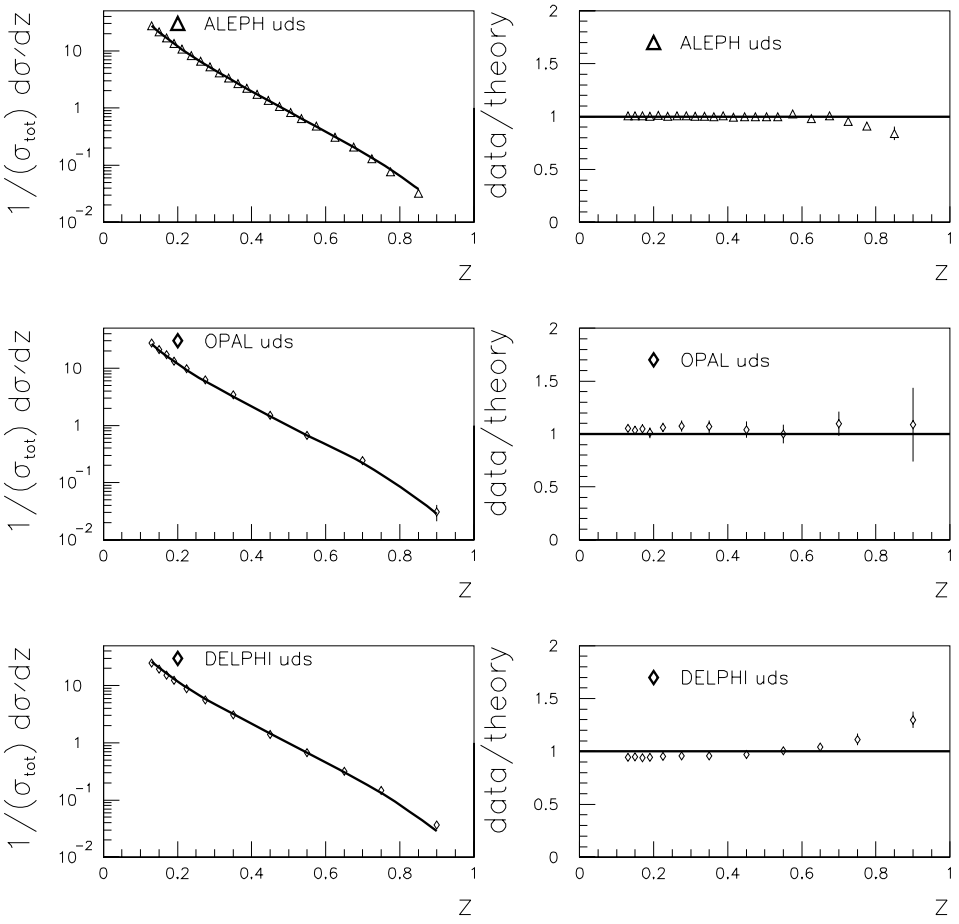

Figure 3: NLO inclusive charged particle production in $e^+e^- \to u, d, sX$ collisions at $\sqrt{s} = 91.2$ GeV with optimized scales and with fragmentation functions obtained here (formula 8) compared to data of the ALEPH [17], OPAL [26] and DELPHI [25] collaboration.

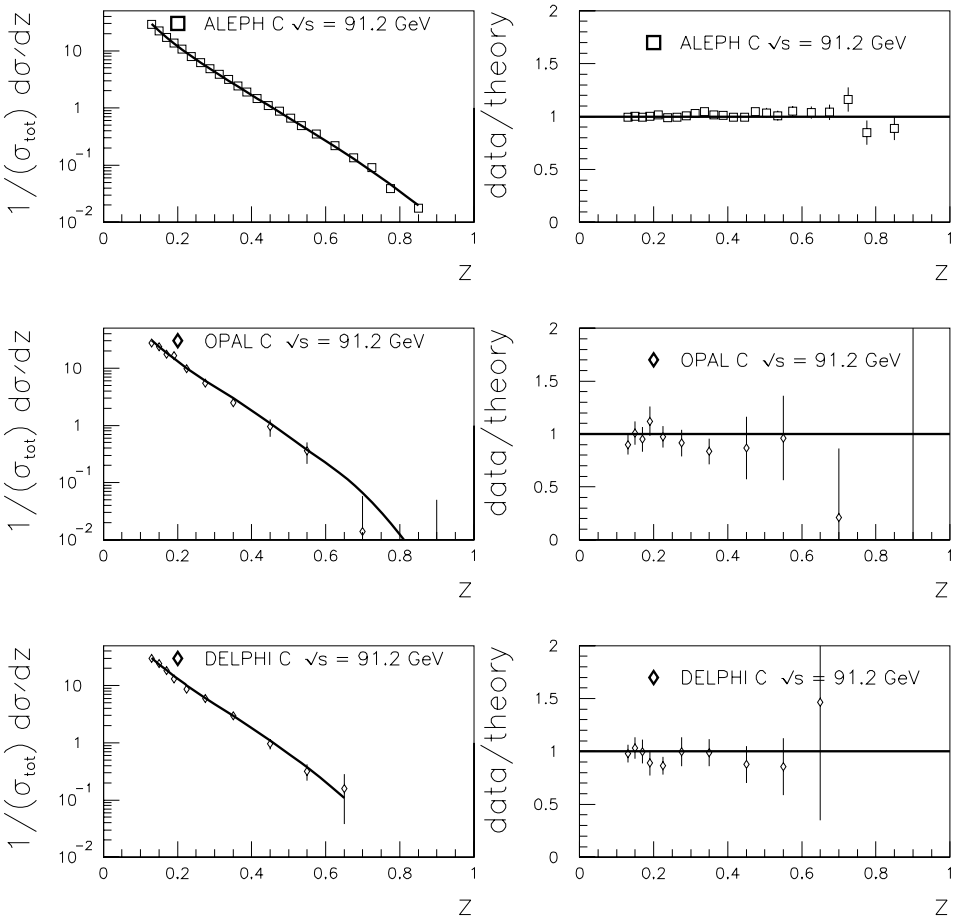

Figure 4: NLO inclusive charged particle production in $e^+e^- \to cX$ collisions at $\sqrt{s} = 91.2$ GeV with optimized scales and with fragmentation functions obtained here (formula 8) compared to data of the ALEPH [17], OPAL [26] and DELPHI [25] collaboration.

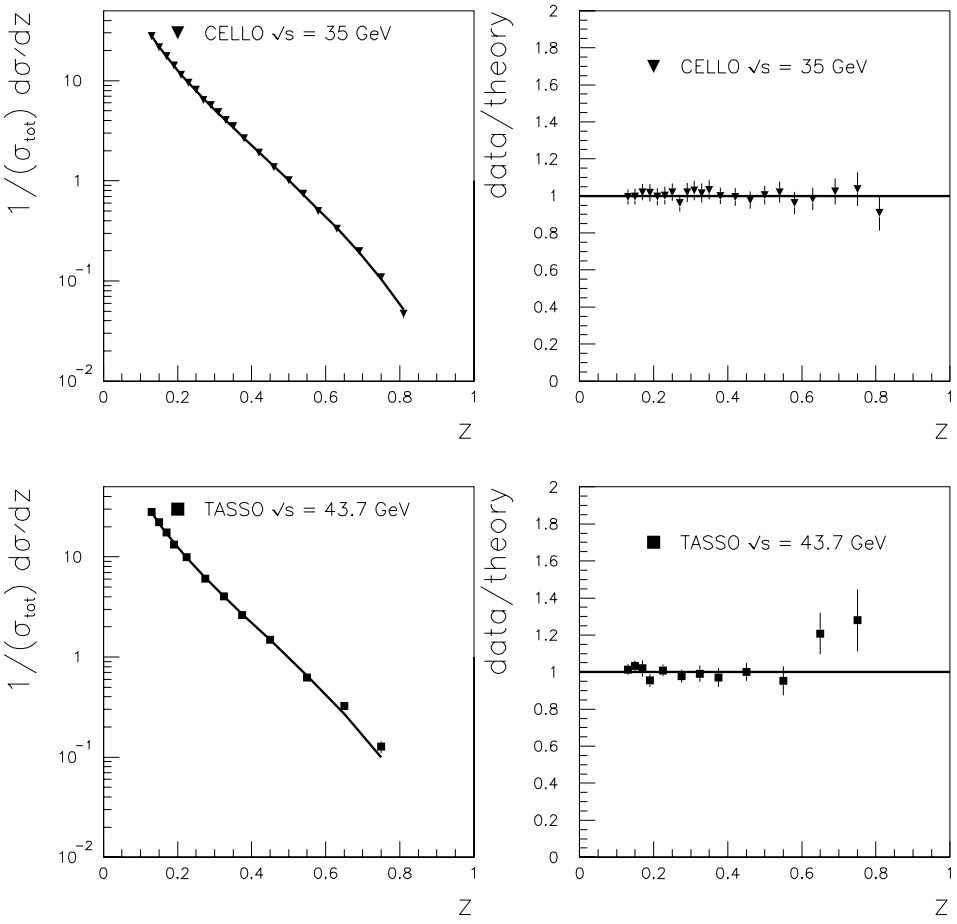

Figure 5: NLO inclusive charged particle production in $e^+e^- \to hX$ collisions with optimized scales and with fragmentation functions obtained here (formula 8) compared to data at $\sqrt{s} = 35$ GeV from the CELLO collaboration [20] and at $\sqrt{s} = 44$ GeV from the TASSO collaboration [21].

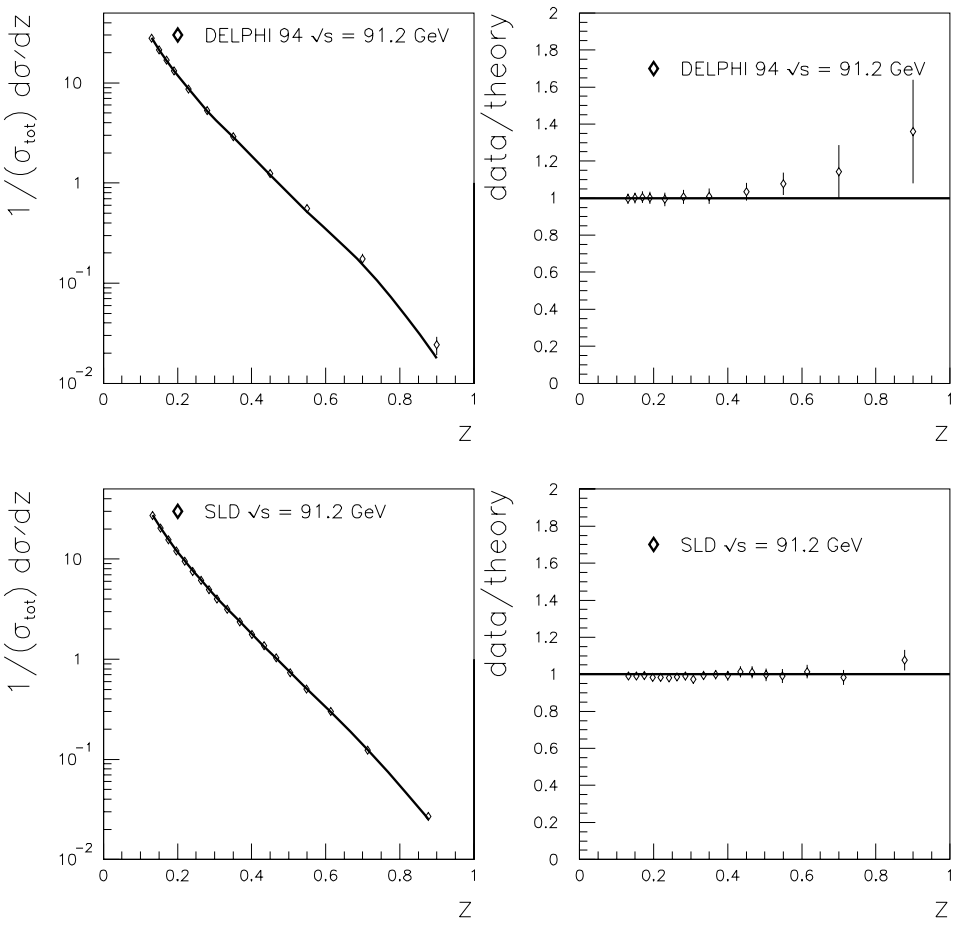

Figure 6: NLO inclusive charged particle production in $e^+e^- \to hX$ collisions at $\sqrt{s} = 91.2$ GeV with optimized scales and with fragmentation functions obtained here (formula 8) compared to data of the DELPHI [23] and SLD [24] collaboration.

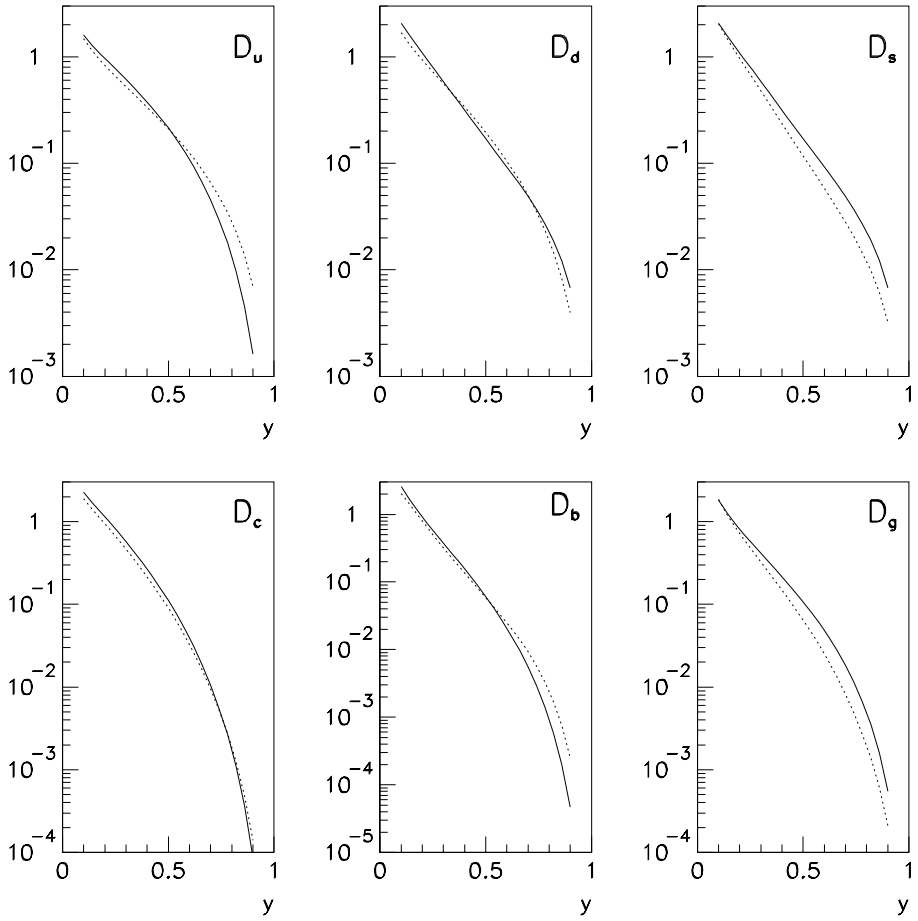

Figure 7: Quark and gluon fragmentation functions obtained in this paper (solid line) are compared at the scale $Q^2 = 10000$ GeV^2 to those obtained by BKK [4] (dotted line).

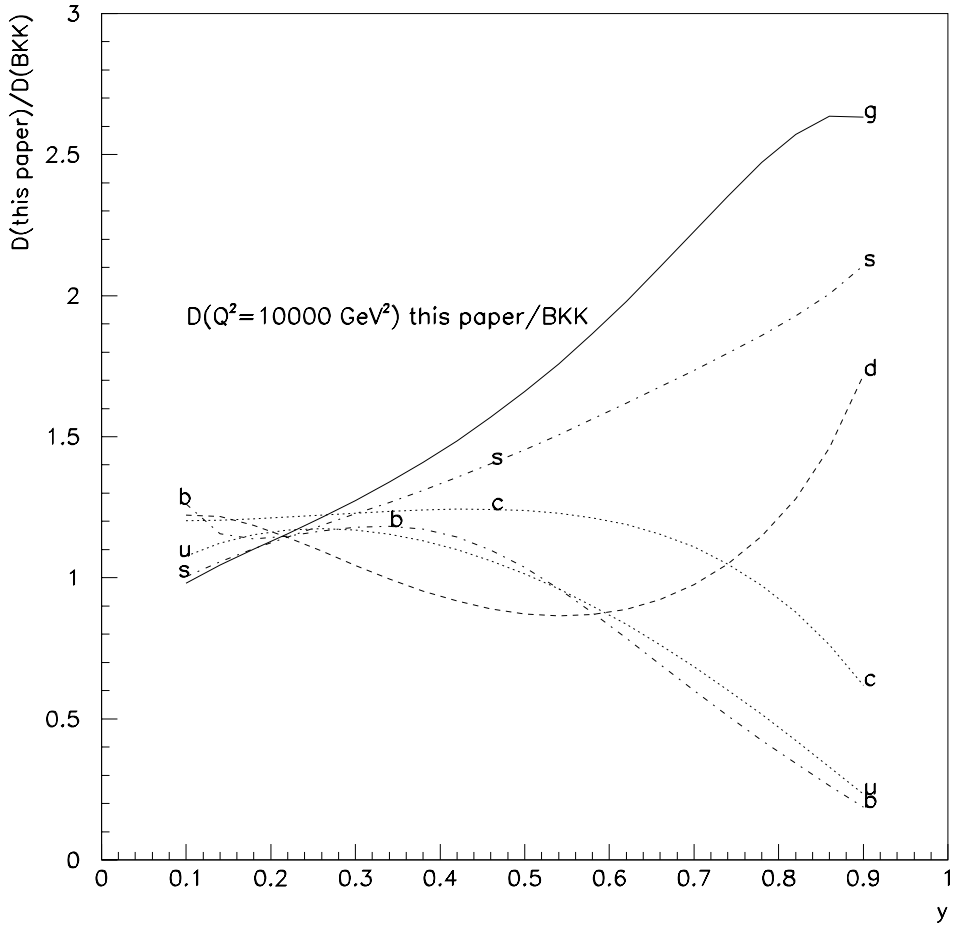

Figure 8: Ratios of the parton fragmentation functions obtained in this paper (formula 8) to those obtained by BKK [4]. The scale is $Q^2 = 10000$ GeV^2.

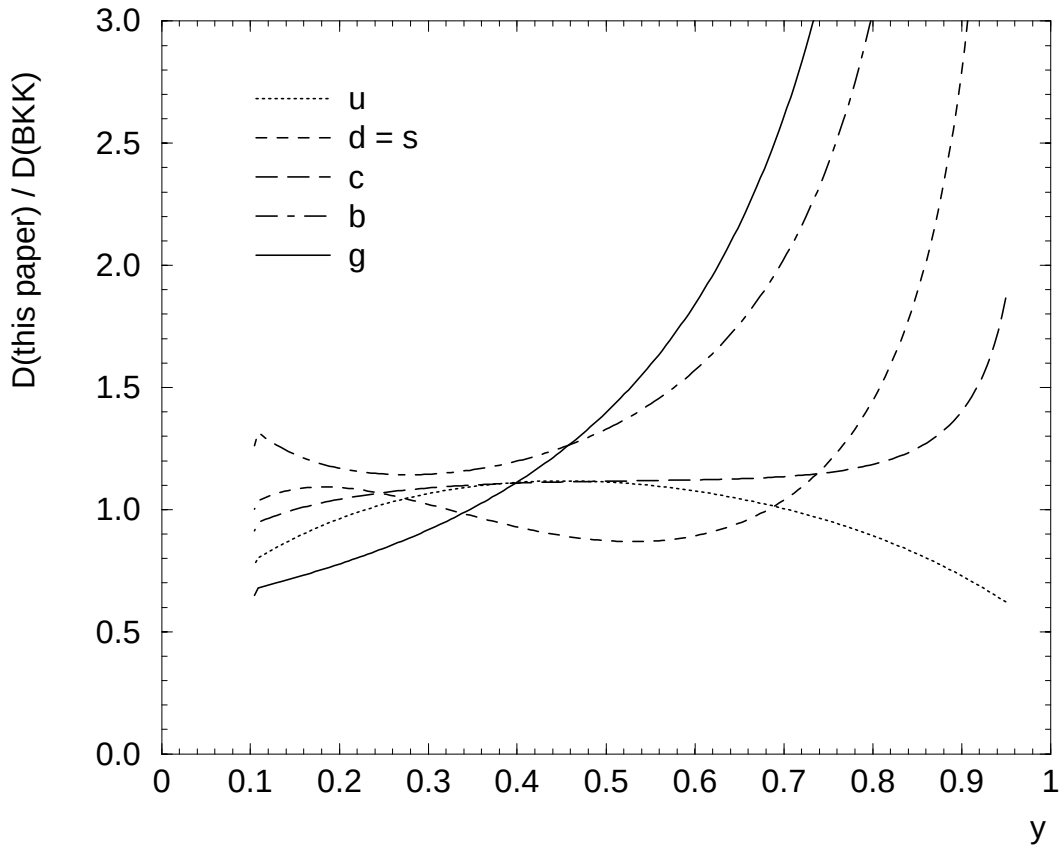

. .

Figure 9: Quark fragmentation functions obtained in this paper (solid line) are compared at the scale $Q^2 = 10000$ GeV^2 to those obtain in [30] using all charged (dotted line).

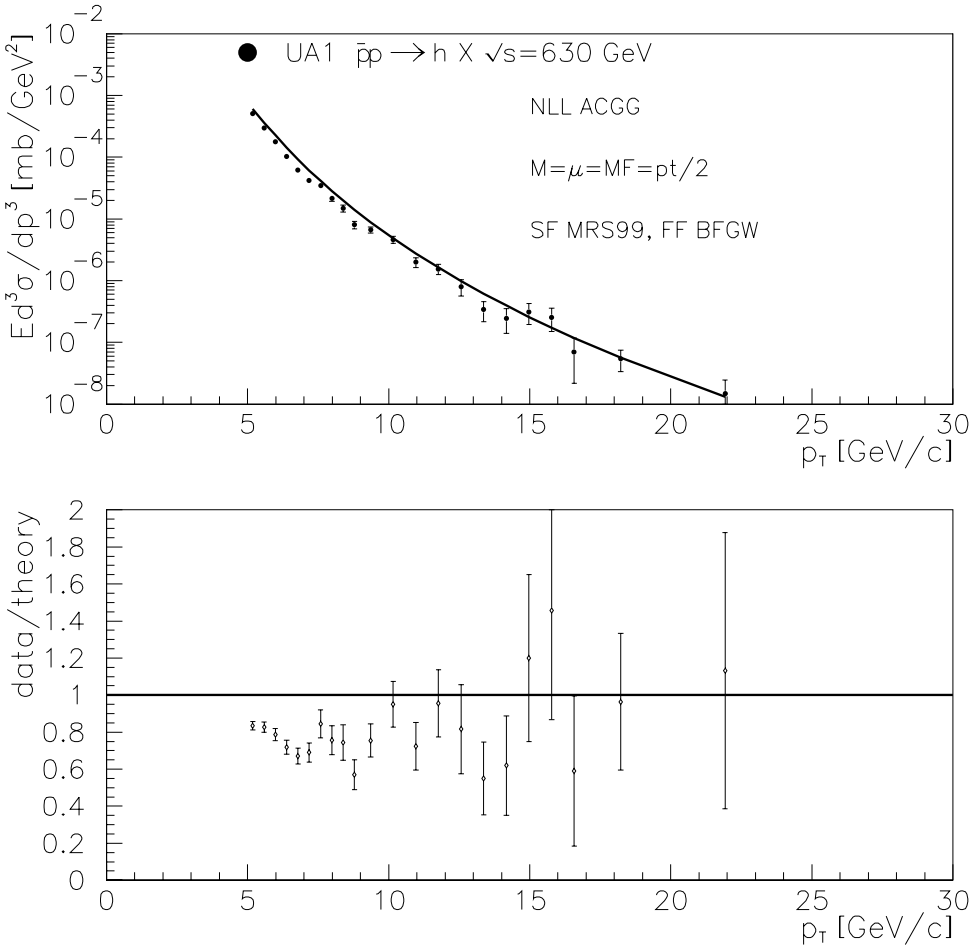

Figure 10: NLO inclusive charged particle production in $p\bar{p}$ collisions at $\sqrt{s}$ = 630 GeV for $\mu = M = M_F = p_T/2$ with fragmentation functions obtained here (formula 8) and structure functions MRS99-2 [19] compared to data of the UA1 collaboration [16].

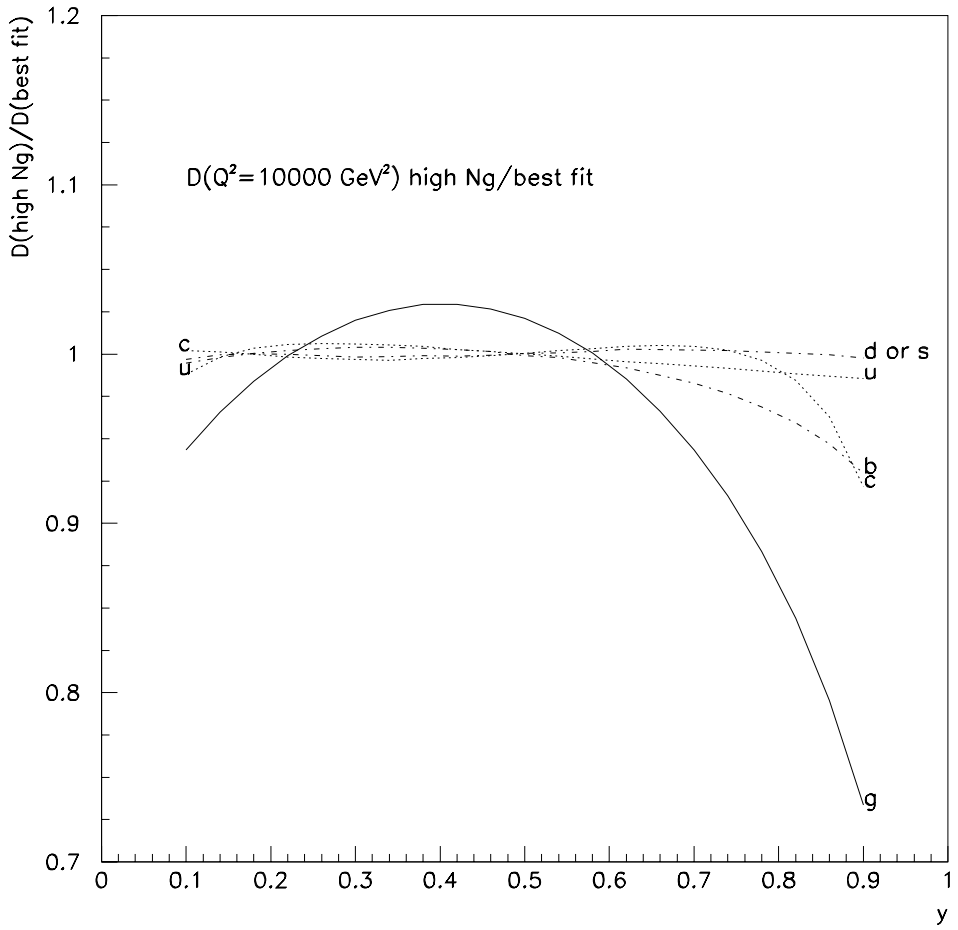

Figure 11: Ratio of the fragmentation functions given by (9) to those of the best fit (8) at the scale $Q^2 = 10000$ GeV^2.

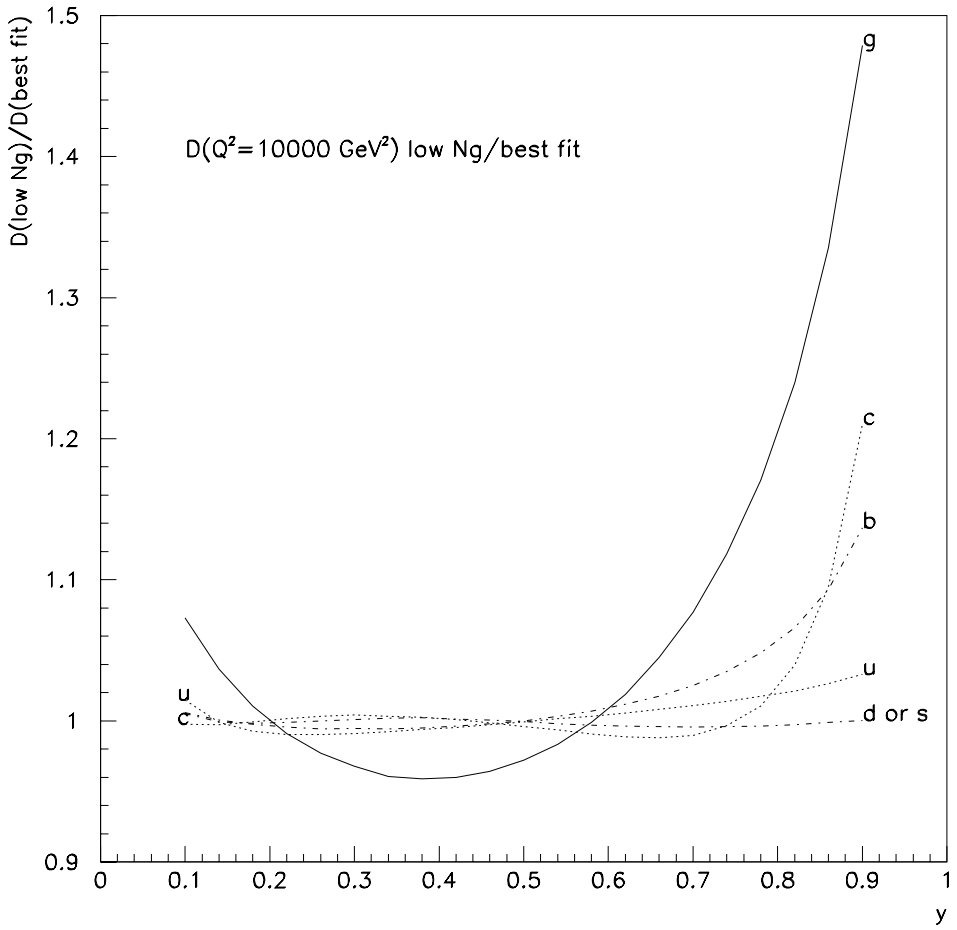

Figure 12: Ratio of the fragmentation functions given by (10) to those of the best fit (8) at the scale $Q^2 = 10000$ GeV^2.

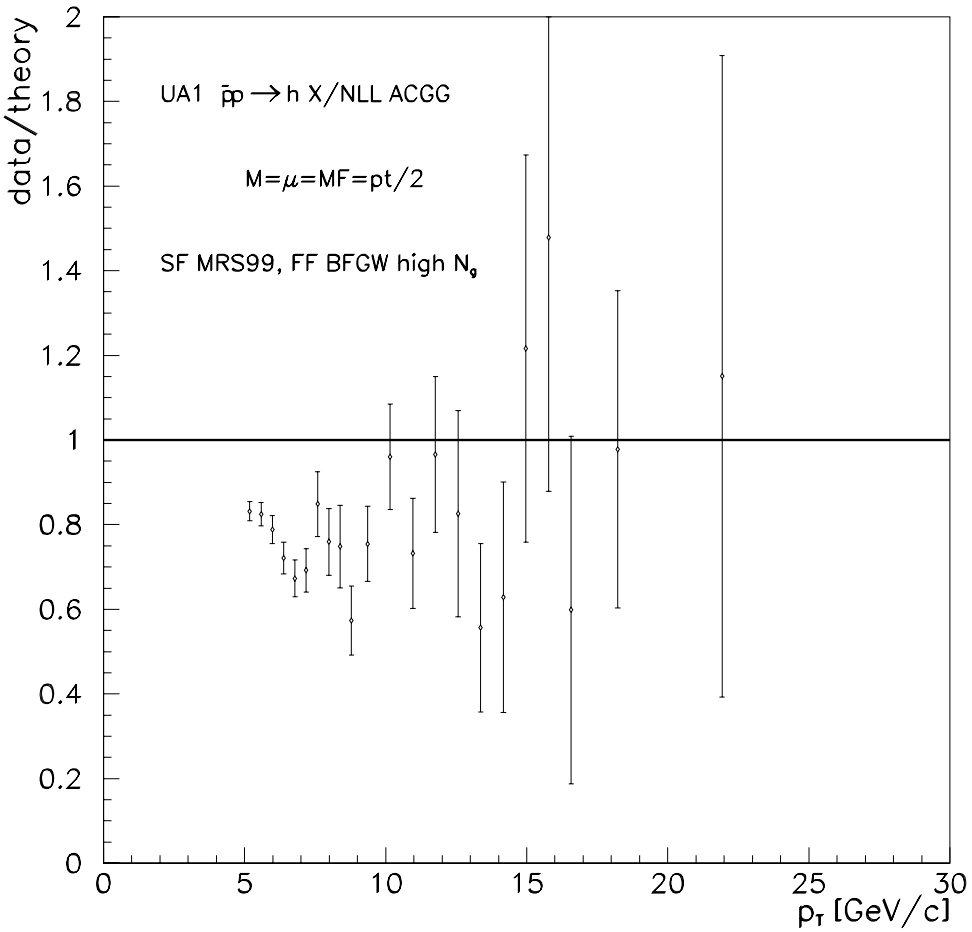

Figure 13: NLO inclusive charged particle production in $p\bar{p}$ collisions at $\sqrt{s} = 630$ GeV for $\mu = M = M_F = p_T/2$ with the set of fragmentation functions obtained here (9) by allowing a $\Delta\chi^2$ of 1 to the best fit and structure functions MRS99-2 [19] compared to data of the UA1 collaboration [16].

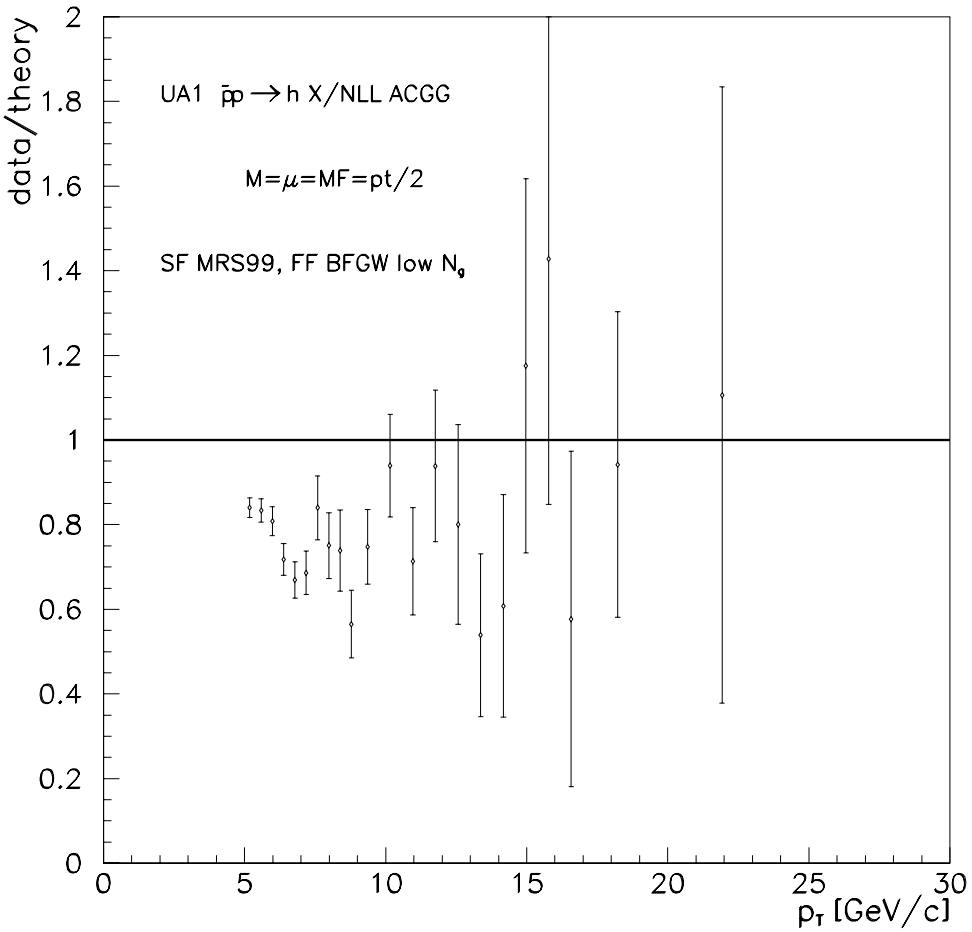

Figure 14: NLO inclusive charged particle production in $p\bar{p}$ collisions at $\sqrt{s} = 630$ GeV for $\mu = M = M_F = p_T/2$ with the set of fragmentation functions obtained here (10) by allowing a $\Delta\chi^2$ of 1 to the best fit and structure functions MRS99-2 [19] compared to data of the UA1 collaboration [16].